Restricted expression of *cdc25a* in the tailbud is essential for formation of the zebrafish posterior body

Cortney M. Bouldin, Corey D. Snelson, Gist H. Farr III,[1] and David Kimelman[2]

Department of Biochemistry, University of Washington, Seattle, Washington 98195, USA

The vertebrate body forms from a multipotent stem cell-like progenitor population that progressively contributes newly differentiated cells to the most posterior end of the embryo. How the progenitor population balances proliferation and other cellular functions is unknown due to the difficulty of analyzing cell division in vivo. Here, we show that proliferation is compartmentalized at the posterior end of the embryo during early zebrafish development by the regulated expression of *cdc25a*, a key controller of mitotic entry. Through the use of a transgenic line that misexpresses *cdc25a*, we show that this compartmentalization is critical for the formation of the posterior body. Upon misexpression of *cdc25a*, several essential T-box transcription factors are abnormally expressed, including Spadetail/Tbx16, which specifically prevents the normal onset of *myoD* transcription, leading to aberrant muscle formation. Our results demonstrate that compartmentalization of proliferation during early embryogenesis is critical for both extension of the vertebrate body and differentiation of the multipotent posterior progenitor cells to the muscle cell fate.

[*Keywords*: proliferation; differentiation; progenitor; somitogenesis; gastrulation; cdc25]

Supplemental material is available for this article.

Received October 22, 2013; revised version accepted January 3, 2014.

From the onset of embryonic development, the single-cell blastomere proliferates numerous times to create a fully formed embryo. However, proliferation needs to be carefully integrated with many other events occurring within the embryo, such as differentiation, intercellular signaling, and morphogenesis. How these different processes are integrated in the embryo remains largely unknown. A dramatic example of the intricate regulation of the cell cycle during embryogenesis was provided by the landmark study of Foe (1989). In gastrulating *Drosophila* embryos, proliferation occurs in highly reproducible mitotic domains (Foe 1989), which represent different compartments of cell fate commitment (Foe 1989; Cambridge et al. 1997). Subsequent work revealed that expression of *string*, a Cdc25-related protein, drives cells into mitosis within these domains (Edgar and O'Farrell 1989, 1990). Although ubiquitous expression of *string* has surprisingly little effect on cell commitment within a developing embryo (Edgar and O'Farrell 1990), forcing mitosis in gastrulating mesoderm is highly disruptive, suggesting that mitosis and morphogenesis are incompatible (Foe et al. 1993). In support of this idea, transcription of the *string* ortholog *cdc25* in the epidermis of the ascidian *Ciona intestinalis* must be carefully controlled for neural tube closure (Ogura et al. 2011). Similarly, Tribbles, which regulates String proteolysis, is necessary for gastrulation in *Drosophila* (Grosshans and Wieschaus 2000; Mata et al. 2000; Seher and Leptin 2000).

In vertebrate embryos, regulation of the entry into mitosis is also essential for normal morphogenesis. In the previously studied vertebrate examples, the function of the kinase Wee1 that opposes the function of Cdc25 (Leise and Mueller 2002; Murakami et al. 2004) or Tribbles-related proteins that control Cdc25 protein levels (Saka and Smith 2004) were required for the morphogenetic movements of gastrulation. Taken together, studies in both invertebrates and vertebrates demonstrate that Cdc25 activity needs to be carefully regulated in order for particular morphogenetic events to occur normally.

During formation of the vertebrate body, newly differentiated cells are continually added to the most posterior end, resulting in an embryo that grows from anterior to

[1]Present address: Center for Developmental Biology and Regenerative Medicine, Seattle Children's Research Institute, Seattle, WA 98101, USA.
[2]Corresponding author
E-mail kimelman@uw.edu
Article published online ahead of print. Article and publication date are online at http://www.genesdev.org/cgi/doi/10.1101/gad.233577.113.

© 2014 Bouldin et al. This article is distributed exclusively by Cold Spring Harbor Laboratory Press for the first six months after the full-issue publication date (see http://genesdev.cshlp.org/site/misc/terms.xhtml). After six months, it is available under a Creative Commons License (Attribution-NonCommercial 3.0 Unported), as described at http://creativecommons.org/licenses/by-nc/3.0/.

posterior. Multipotent cells, preserved at the posterior end of the embryo in a region called the tailbud, drive this process (for review, see Wilson et al. 2009). As the embryo extends during the somite-forming stages, some cells commit to leave the tailbud and become mesodermal or neural cells, and some remain bipotential to contribute to more posterior tissue. Proliferation occurs as the embryo extends (Kanki and Ho 1997; Cambray and Wilson 2002; Tzouanacou et al. 2009), whereas inhibiting proliferation in vertebrates results in truncated embryos (Cooke 1973; Tam 1981; Zhang et al. 2008). Depending on when proliferation is blocked, either somites are lost (Cooke 1973) or a similar number of smaller somites are formed (Tam 1981). Little is known about how proliferation progresses during posterior body formation because of the difficulties associated with analyzing proliferation in a constantly changing multicellular embryo. For instance, a previous study in zebrafish examined proliferation in multiple cell types using dye injection of blastomeres followed from the start of gastrulation, but only a single cell that contributes to the more posterior mesoderm of the embryo was labeled and followed (Kimmel and Warga 1987).

Recent advances in lineage analysis using photoconvertible proteins (for review, see Buckingham and Meilhac 2011) allow a single cell to be efficiently targeted and followed for individual cell divisions using time-lapse imaging. The bipotential cells that contribute to the posterior body in zebrafish make an excellent model for in vivo analysis of proliferation during anterior–posterior growth because the precise location of the cells is known from the time of initial specification until final differentiation (Kimmel et al. 1990; Kanki and Ho 1997; Warga and Nusslein-Volhard 1999), they are readily accessible for visualization and manipulation, and the general mechanism for posterior extension of the body is conserved among vertebrates (Kanki and Ho 1997).

In zebrafish, as in other vertebrates, the progenitors move through a defined series of transcriptional changes as they progress from the bipotential neural/mesodermal state to differentiated muscle (Griffin and Kimelman 2002; Martin and Kimelman 2012), although with some relatively minor species-specific differences in the transcription factors that are used (Fig. 7A, below; Lardelli 2003; Ahn et al. 2012). Common to all vertebrates is the expression of Brachyury (called No tail [Ntl] in zebrafish) (Schulte-Merker et al. 1994), an essential T-box gene that maintains the progenitors in the bipotential state through the regulation of Wnt signaling (Martin and Kimelman 2008, 2010, 2012). As cells first begin to differentiate along the mesodermal lineage in zebrafish, they activate the T-box factor Tbx16/Spadetail (Spt; the functional equivalent of mammalian Tbx6) and Mesogenin (Row et al. 2011; Fior et al. 2012; Yabe and Takada 2012) in a region that we previously referred to as the maturation zone (Griffin and Kimelman 2002). After exiting the maturation zone, cells cease expressing *ntl* and continue to differentiate as they enter the presomitic mesoderm (PSM), where the cells are subdivided by a molecular clock and wave front into epithelialized blocks called somites (for review, see Holley 2007; Pourquié 2011; Oates et al. 2012). Cells of the somite can then produce several types of tissues, including bone, dermis, and muscle (for review, see Christ et al. 2007), although, in the early zebrafish embryo, muscle is by far the major derivative of the somites. Differentiation of muscle requires the activity of the myogenic regulatory factors (MRFs) that are capable of inducing muscle differentiation de novo (for review, see Tapscott 2005; Buckingham and Vincent 2009). In zebrafish, MyoD and Myf5 are the essential MRFs of the early embryo (Hinits et al. 2009). These transcription factors provide important landmarks for the differentiation state of the mesodermal cells.

In this study, we identified the timing and location of the posterior progenitor cell divisions. Our results show that proliferation is not continuous but is markedly different between gastrulation, when the cells divide rapidly, and somitogenesis, when they enter an extended interphase before adopting the mesodermal fate and dividing. We show that the extended interphase is due to the acquisition of an extended S/G2 phase, which corresponds to the loss of expression of the key checkpoint gene *cdc25a* specifically from the posterior progenitors during somitogenesis. Through timed misexpression of Cdc25, we demonstrate that restricted expression of Cdc25 is required during the somite-forming stages for muscle cell differentiation, not simply for morphogenesis of the posterior body. We show that cell cycle alteration causes a cell-autonomous perdurance of *spt* expression, which prevents the onset of *myoD* and *myf5* in the PSM, resulting in a deficit of muscle cells along the posterior body. Our results reveal an unexpected link between the precise regulation of the S/G2 phase of the cell cycle and differentiation from multipotency in vivo.

Results

Proliferation in early zebrafish embryos occurs in two phases

By the start of gastrulation in zebrafish, the mesodermal territory that will form the complete body axis has been specified in a region located at the margin between the cells of the animal pole and the yolk of the vegetal pole (Kimmel et al. 1990; Schier and Talbot 2005; Kimelman 2006). Whereas the bulk of the mesoderm forms the anterior somites, a small number of progenitors located at the ventral margin are fated to contribute to the entire posterior half of the body (somites 16–34) (Warga and Nusslein-Volhard 1999; Szeto and Kimelman 2006), necessitating cell proliferation. To study the proliferation of these posterior progenitor cells, we produced a new transgenic zebrafish line ubiquitously expressing a photoconvertible protein targeted to the nucleus (EF1α:NLS-Kikume) and then labeled single cells by targeting them with a short pulse of ultraviolet light, which photoconverts Kikume from green to red (Tsutsui et al. 2005).

We began by investigating proliferation of the posterior progenitors during the gastrula stages, from their initial specification at the ventral margin at the start of gastrulation (~6 h post-fertilization [hpf]) until the completion

of gastrulation and the formation of the tailbud (~12 hpf). By static and time-lapse imaging, we most commonly observed that each labeled cell produced four progeny within this time frame, indicating that the originally labeled cell had divided twice (Supplemental Fig. S1). Interestingly, daughter cells of a single labeled cell divided within 30 min of each other, indicating synchrony between daughter cells. These results are consistent with previous observations of general mesodermal proliferation during gastrulation (Kane et al. 1992) and indicate that the posterior progenitors behave similarly to cells destined for the anterior somites during this 4-h time frame.

Our principle interest was in proliferation of progenitor cells during the somitogenesis stages. By the end of gastrulation, the tailbud is a concentrated mass of progenitor cells (Kanki and Ho 1997), making it very difficult to photoconvert single cells; however, we reasoned that at 90% epiboly, the posterior progenitor cells would be spread along the ventral side of the embryo in a thin sheet, making single cells easier to target. To test this, we photoconverted cells at specific distances from the blastopore and subsequently imaged them after completion of somitogenesis. Not only were we able to easily label single cells using this approach but we also found that the distance the progenitor cells were located from the blastopore correlated with position along the anterior–posterior axis (Fig. 1A). In particular, cells located 20 cell diameters from the blastopore consistently contributed to the most posterior somites, which is particularly useful for long-term imaging of the progenitors during somitogenesis.

To examine proliferation, we labeled the posterior progenitors at 90% epiboly and followed them until the completion of somitogenesis by continuous time-lapse imaging (Fig. 1B). We observed that each of the progenitors underwent a single division over 8 h of observation during the somitogenesis stages (Fig. 1C). Importantly, we found that although the progenitor cells actively divided during the gastrula stages, they were quiescent while in the progenitor zone during somitogenesis. Following the division, both daughter cells exited the tailbud and entered the PSM, indicating that each of the progenitor divisions was a symmetric division, not an asymmetric division that caused one cell to differentiate and left one cell in the progenitor population.

Significantly, we observed that the location of the dividing cells is very consistent. Cells underwent the division soon after they migrated from the dorsal to the ventral part of the tailbud (Fig. 1B; Supplemental Movie S1), which is the first overt sign of differentiation (Fior et al. 2012; Lawton et al. 2013). Thus, the variation in the timing of progenitor cell division that we observed during somitogenesis in Figure 1C correlates with the variation in time for specific progenitor cells to begin the process of differentiation, suggesting a tight coupling between proliferation and differentiation.

Posterior progenitors are held in the S or G2 phase of the cell cycle

Our labeling results revealed that the posterior progenitors divide rapidly during the gastrula stages but then enter a prolonged quiescence during somitogenesis until they begin to differentiate. Next, we wished to identify where in the cell cycle the posterior progenitors were held during their quiescent phase. Fluorescent ubiquitin-mediated cell cycle indicator (FUCCI) is a unique tool that uses the cyclical turnover of cell cycle proteins to indicate the phase of the cell cycle in living cells (Sakaue-Sawano et al. 2008). Cells in S, G2, or M phase express a green fluorescent protein (GFP), whereas cells in G1 ex-

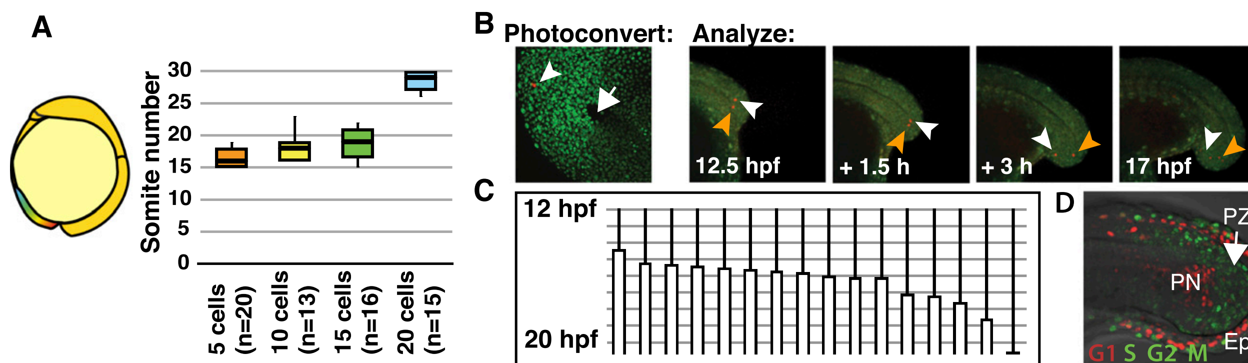

Figure 1. Progenitors that contribute to the posterior-most body divide once during somitogenesis. (*A*) Cells were photoconverted at a set distance from the blastopore, and the fate along the anterior–posterior axis was recorded (in somite number on the *Y*-axis ,with 1 being the anterior-most and 30 being the posterior-most somite; the *X*-axis is the number of cell diameters from the blastopore). Cells 20 cell diameters from the blastopore contribute to the most posterior somites. (*B*) NLS-Kikume in a single nucleus 20 cells from the blastopore was photoconverted at 9 hpf. In this example, the cell underwent a division before the start of somitogenesis. Time-lapse images of the two labeled daughter cells show that cells divided once after they moved into the ventral part of the tailbud. Arrowheads mark labeled cells, and the arrow marks the blastopore. White and orange arrowheads mark different labeled cells. See also Supplemental Movie S1. (*C*) Cell lineage maps from time-lapse imaging of 17 labeled cells revealed that cell division occurred once over a period of 8 h during somitogenesis. (*D*) The Dual Fucci transgene reveals that nondividing cells in the progenitor zone (PZ) are in the S, G2, or M phases (green). These cells can be contrasted with the posterior notochord (PN) and epidermal cells (Ep) that are mostly in G1 (red). See also Supplemental Figure S2 and Supplemental Movie S2.

press a red fluorescent protein. FUCCI was recently adapted for use in zebrafish (Sugiyama et al. 2009) but is limited because it requires crossing two different hemizygotes to create embryos with the two indicator transgenes, meaning that only one-quarter of the embryos are useful for analysis. To address this limitation, we created a new transgenic line, Dual Fucci, which simultaneously expresses both indicators bicistronically using a viral 2A peptide (Provost et al. 2007). In addition, we placed this construct under the control of the *ubiquitin* promoter, which, unlike the *EF1α* promoter used in the original transgenic lines that is silenced after a few days of development, remains active throughout development and into adulthood (Mosimann et al. 2011), significantly expanding the utility of FUCCI in zebrafish. Using Dual Fucci, we determined that the posterior progenitors are in the S, G2, or M phase during somitogenesis (Fig. 1D). Since the cells do not divide until they leave the progenitor zone, they are not undergoing mitosis and so must be held in S or G2.

The key innovation of the FUCCI system is that it allows analysis of the cell cycle in living embryos. If the bipotential posterior progenitor cells are held in the S or G2 phase of the cell cycle until differentiation, we would predict that a population of green cells would be maintained in the tailbud until somitogenesis is completed. To follow the cell cycle of the posterior progenitors throughout the course of somitogenesis, we imaged Dual Fucci transgenic embryos over time. A population of green cells was maintained at the tip of the tail in the posterior progenitor zone (Supplemental Fig. S2; Supplemental Movie S2). Intriguingly, the completion of somitogenesis coincided with depletion of green cells from the tip of the tail. In summary, still and time-lapse imaging of Dual Fucci embryos indicates that posterior progenitor cells are held either in S phase or at the G2/M transition.

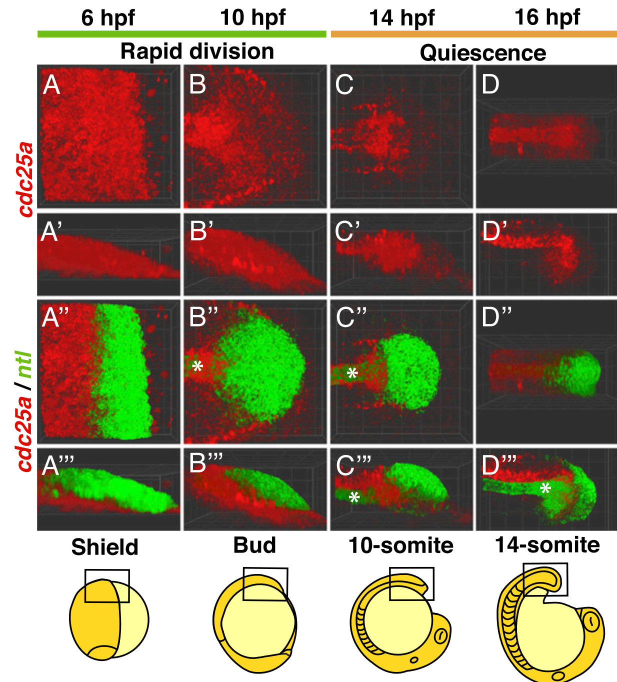

Figure 2. Two phases of proliferation coincide with two phases of expression of the mitotic phosphatase *cdc25a*. Three-dimensional (3D) projections of fluorescent whole-mount in situ hybridizations at four developmental stages reveal that *cdc25a* (red) is expressed broadly within the posterior progenitors at shield (*A–A‴*) and tailbud (*B–B‴*) stages. (*C–D‴*) During somitogenesis, *cdc25a* expression is cleared from the tailbud. The progenitor cells are marked by the expression of *ntl* (green), which also is expressed in the notochord (*) in more anterior regions. Cartoons depict the stage and orientation of the embryos, and the boxes depict the region photographed. *A–D* and *A″–D″* are surface views of the embryo, whereas *A′–D′* and *A‴–D‴* are cross-sectional views.

Cdc25a *is not expressed by the posterior progenitors*

Cdc25 is a conserved phosphatase that drives cells into mitosis (Russell and Nurse 1986; Gautier et al. 1991; Dalle Nogare et al. 2007). Because Cdc25 plays a central role in remodeling the cell cycle of the early embryo (Edgar and Datar 1996; Shimuta et al. 2002; Dalle Nogare et al. 2009; DiTalia et al. 2013; Farrell and O'Farrell 2013) and loss of zygotic Cdc25a in zebrafish bends and shortens the axis (Verduzco et al. 2012), we investigated the expression of *cdc25* in the posterior progenitor cells using fluorescent in situ hybridization. Zebrafish have two *cdc25* orthologs: *cdc25a* and *cdc25d* (Dalle Nogare et al. 2007). *cdc25d* is weakly expressed and ubiquitous during somitogenesis (Dalle Nogare et al. 2007; data not shown). To examine the expression of *cdc25a* in the progenitor zone, we coexamined *ntl*, which marks the progenitor population (Martin and Kimelman 2010, 2012). During the gastrula stages, when the progenitors are rapidly dividing, *cdc25a* is expressed throughout the progenitor cells (Fig. 2A–B‴). In contrast, during somitogenesis, when the progenitors become quiescent, *cdc25a* is excluded from the posterior progenitors and expressed by cells that have exited the progenitor zone (Fig. 2C–D‴). Thus, the expression of *cdc25a* during gastrulation and somitogenesis is consistent with the rapid proliferation of the progenitors during the gastrula stages and the initiation of a prolonged G2 phase in somitogenesis.

Ectopic expression of cdc25a *results in loss of somites and muscle fibers*

Exclusion of *cdc25a* from the posterior progenitor cells led us to hypothesize that absence of Cdc25a was important for extending the interphase of the posterior progenitors and consequently essential for axis elongation. To test these hypotheses, we sought to express *cdc25a* throughout the embryo. Ectopic expression of *cdc25a* mRNA in early embryos causes lethality (Dalle Nogare et al. 2007). Misexpression of Cdc25 using a heat-shock promoter has been widely used in *Drosophila* to study its effects on early embryogenesis (Edgar and O'Farrell 1990; DiTalia and Wieschaus 2012; Farrell et al. 2012). To circumvent early embryo lethality, we created a transgenic zebrafish line that used a heat-shock promoter to drive both *cdc25a* and the fluorescent marker *venus*

throughout the embryo. The transgene is referred to here as *hsp70:cdc25.*

To examine the phenotypic effects of ectopic Cdc25a, we heat-shocked *hsp70:cdc25* embryos midway through somitogenesis (12-somite stage) and allowed embryos to finish axis elongation. We chose this time because it allowed us to examine the effects on somites that had already formed and cells that had completely differentiated versus cells that were still in the progenitor and early differentiation states. Ectopic Cdc25a caused an increase in cell death, which was eliminated by injecting a p53 morpholino oligonucleotide (MO) (Supplemental Fig. S3). The p53 MO itself has no effect on embryo development (Fig. 3B; Robu et al. 2007). Embryos with ectopic Cdc25a that had been injected with p53 MO were classified into three phenotypes that were present at approximately equal levels (Supplemental Fig. S4). Embryos with the strongest phenotype (P3) were much shorter, with bent axes and smaller heads (Fig. 3B). Embryos with the P3 phenotype were used in subsequent analyses. We also confirmed that, as expected, misexpression of Cdc25 caused a twofold increase in the mitotic index in the tailbud (Fig. 3A; Supplemental Fig. S3). These data establish that ectopic Cdc25a forces the posterior progenitors into mitosis, spatial restriction of Cdc25a maintains a quiescent progenitor state, and alteration of this quiescent state leads to perturbations in posterior body formation.

To investigate the effect of ectopic Cdc25a further, we looked at somite number, somite shape, and cross-sectional area of the myotome. Transgenic embryos with the strongest phenotype formed an average of 14 somites after heat shock, which represented an average loss of seven somites after a 12-somite heat shock ($P < 0.001$) (Fig. 3C). This was not a failure of the PSM to segment somites, since we could see somite boundaries at the most posterior end of the body. However, the posterior somites were clearly abnormal, with narrower somites along the anterior–posterior axis and a 66% reduction in the mean cross-sectional area of the myotome, indicating a loss of muscle mass ($P < 0.001$) (Fig. 3D–G; data not shown). These results demonstrate that ectopic Cdc25a prevents normal axis extension and somite formation and suggest that the defects are not simply due to alterations in morphogenesis.

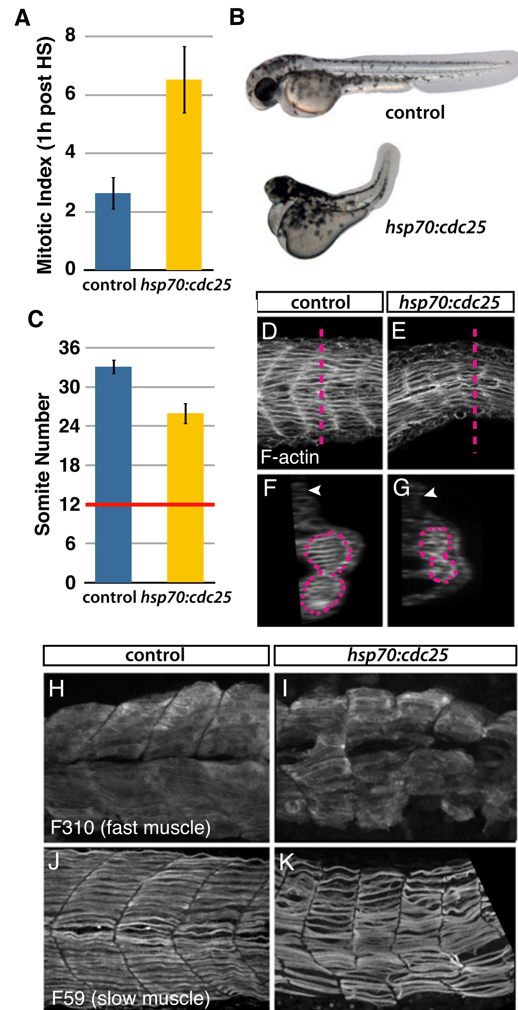

Figure 3. Ectopic expression of *cdc25a* disrupts posterior body formation and muscle differentiation. (*A*) Mean mitotic index increased in embryos with the *hsp70:cdc25* transgene 1 h after heat shock (error bars represent one standard deviation; $P < 0.01$). (*B*) Bright-field images revealed truncation of the posterior body and reduced head size after ectopic expression of *cdc25a*. (*C*) Embryos lost an average of seven somites after ectopic expression of *cdc25a* (error bars represent one standard deviation; $P < 0.001$). The red line marks the number of somites formed before the heat shock. (*D*,*E*) F-actin staining shows abnormal somite shape in a lateral view. The dashed pink line marks the 22nd somite. (*F*,*G*) Cross-section of somite 22 from *D* and *E* shows that dorsal and ventral compartments are formed but reduced in size. Arrowheads highlight the dorsal fin, and the myotome is outlined with a dashed pink line. (*H*,*I*) Fast muscle, detected by F310 immunofluorescence, was aberrant after ectopic Cdc25a. (*J*,*K*) Slow muscle fibers, detected by F59 immunofluorescence, were wavy and unevenly spaced after *cdc25a* expression. Embryos were heat-shocked at the 12-somite stage. All embryos were injected with 1 ng of the p53 MO. See also Supplemental Figures S3 and S4.

Ectopic Cdc25a disrupts fast and slow muscle fiber formation

In zebrafish embryos, cells that contribute to fast and slow muscle fiber types develop from distinct populations of cells, with the fast muscle cells originating in the progenitor population described above (Devoto et al. 1996; Hirsinger et al. 2004). To analyze the effect of ectopic Cdc25a on fast and slow muscle cells, we analyzed markers of each by immunofluorescence. By carefully examining somite shape, we found that somites first became irregular at the fourth somite formed after the heat shock. Somites posterior to this contained gaps in the fast muscle marker F310 (Fig. 3H,I). Additionally, slow muscle fiber analysis with the marker F59 showed a milder phenotype, with aberrant spacing between slow muscle fibers and wavy morphology (Fig. 3J,K). To complete differentiation, slow muscle cells elongate and migrate laterally through the nascent fast muscle cells (Henry et al. 2005; Hollway et al. 2007; Stellabotte et al. 2007).

Spacing between fibers and wavy morphology of the slow muscle expression could therefore be a result of slow muscle cells migrating through abnormal fast muscle (as in Bessarab et al. 2008).

MyoD and Myf5 are critical for muscle formation in zebrafish (Hinits et al. 2009). We therefore examined their expression to determine whether Cdc25a was affecting early muscle differentiation. For these experiments, we were unable to sort embryos by phenotype, and a mix of all three phenotypes was used. Embryos were heat-shocked at the six-somite stage and harvested 4 h after the heat shock because it is easier to visualize gene expression when the PSM is larger and broader, but the same results were seen with a 12-somite heat shock (data not shown). Slow muscle cells in zebrafish are initially formed along the medial edge of a somite in cells adjacent to the notochord, also known as adaxial mesoderm, whereas fast muscle is produced from a more lateral population (Devoto et al. 1996). After ectopic *cdc25a* expression, expression of *myoD* is reduced in the fast muscle precursors but is at normal levels in the slow muscle precursors (Fig. 4A,B). Expression of *myf5* is reduced in both slow and fast muscle precursors (Fig. 4C,D). Importantly, loss of *myf5* alone does not preclude muscle fiber formation, whereas loss of both *myoD* and *myf5* blocks formation of muscle, consistent with the loss of fast muscle but not slow muscle when *cdc25a* is misexpressed (Hammond et al. 2007; Maves et al. 2007). Together, these data show that cells with ectopic Cdc25a have defects in formation of both fast and slow muscle fibers, with a major reduction in the levels of fast muscle *myf5* and *myoD*.

Ectopic Cdc25a causes misexpression of Spadetail and blocks muscle differentiation

Differentiation of fast muscle from posterior progenitor cells requires stepwise transitions through distinct domains that are marked by the expression of several T-box transcription factors (Fig. 7A, below). The first gene activated at the onset of mesodermal differentiation is *spt*, which is initially coexpressed with *ntl* (Amacher et al. 2002; Griffin and Kimelman 2002). *tbx24* expression follows this and depends on Spt (Nikaido et al. 2002; Row et al. 2011). Following ectopic expression of *cdc25a*, *spt* and *tbx24* transcription is initiated normally, but surprisingly, cells are unable to silence their expression (Fig. 4E–H). We observed a similar but less dramatic perdurance of *spt* and *tbx24* when embryos were heat-shocked at the six-somite stage and left for 4 h (data not shown). These results show that alteration in the cell cycle leads to continued expression of key early differentiation genes. To determine whether ectopic *cdc25a* expression caused all early genes to remain active, we examined the expression of the progenitor marker *ntl*. Unlike *spt* and *tbx24*, *ntl* expression shuts off normally when *cdc25* is ectopically expressed (Fig. 4I–L). Interestingly, we noted that while *ntl* was expressed normally in the progenitor zone (Supplemental Fig. S5), it was diminished in the maturation zone (Figs. 4K,L, 7A [below]). These data show that ectopic Cdc25a blocks the normal progress of differentiation in the mesodermal descendants of the posterior progenitors.

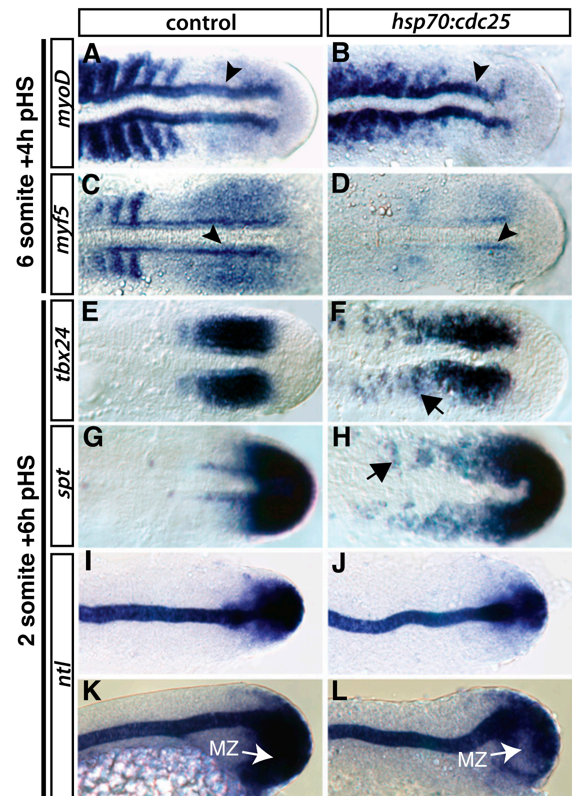

Figure 4. Gene expression is disrupted after *cdc25a* misexpression. (*A*,*B*) *myoD* is reduced in lateral paraxial mesoderm but not adaxial mesoderm after ectopic Cdc25a (80%; *n* = 44). (*C*,*D*) *myf5* is reduced in both fast and slow muscle precursors after Cdc25a misexpression (88%; *n* = 32). Arrowheads in *A*–*D* highlight the adaxial cells. (*E*,*F*) *tbx24* expression expanded after ectopic Cdc25a (90%; *n* = 29). The arrow marks the most recently formed somite, which normally expresses *tbx24*. (*G*,*H*) *spt* expression similarly expanded after Cdc25a misexpression (89%; *n* = 46). Cells within somites that maintain *spt* expression are marked with an arrow. (*I*–*L*) *ntl* expression was reduced after ectopic Cdc25a expression (63%, *n* = 54). (*K*,*L*) The lateral view shows that the ventral expression domain of *ntl*, which corresponds to the maturation zone (MZ), is reduced after misexpression of Cdc25a. Embryos were heat-shocked using conditions listed at the *left* of the figure, where post-heat shock is abbreviated as pHS, and all embryos were harvested at the 14-somite stage. All images are dorsal views except *K* and *L*, which are lateral views.

Perduring Spt in the PSM of embryos misexpressing *cdc25a* suggested that the cells remained in an undifferentiated state for a prolonged period, resulting in a failure to differentiate. Spt plays a major role in starting the differentiation program of the mesodermal cells (Kimmel et al. 1989; Ho and Kane 1990; Row et al. 2011), and so we wondered whether failure to silence Spt expression might account for the inability of muscle cells to differentiate. To test this hypothesis, we temporally misexpressed *spt* using the *hsp70* promoter by injecting at the one-cell stage a DNA construct that has Spt fused through a 2A

peptide to NLS-Kikume, which results in both proteins being produced as separate polypeptides. As a control, we used a construct with a multimeric heat-shock element that drives expression of eGFP (Martin and Kimelman 2010). DNA injection in zebrafish embryos produces mosaic expression of proteins, which is useful for studying cell-autonomous effects (Fig. 5A). Following the injection, embryos were heat-shocked at the 12-somite stage and then left to develop for 4 h. Whereas control cells expressing GFP showed normal *myoD* expression, cells with ectopic Spt were incapable of transcribing *myoD* (Fig. 5B–E). Taken together, our data show that misregulation of the cell cycle by altering the normal expression of Cdc25a keeps cells in an immature state through prolonged Spt expression, which prevents normal *myoD* expression and thus normal differentiation of muscle.

Perduring Spadetail is cell-autonomous

Several signaling pathways, including Wnt and Fgf, are involved in specification and differentiation of the most posterior mesoderm (for review, see Kimelman 2006). Prolonged expression of *spt* after ectopic expression of *cdc25a* could be dependent on the extracellular signaling environment or intracellular effects. To determine which was the case, we transplanted *hsp70:cdc25* cells to a wild-type environment and assessed their ability to ectopically produce Spt (Fig. 6A). Cells expressing *cdc25a* also produced Spt ectopically (Fig. 6B–E), demonstrating that ectopic Cdc25a regulates Spt production cell-autonomously and is likely not dependent on changes to the extracellular signaling environment.

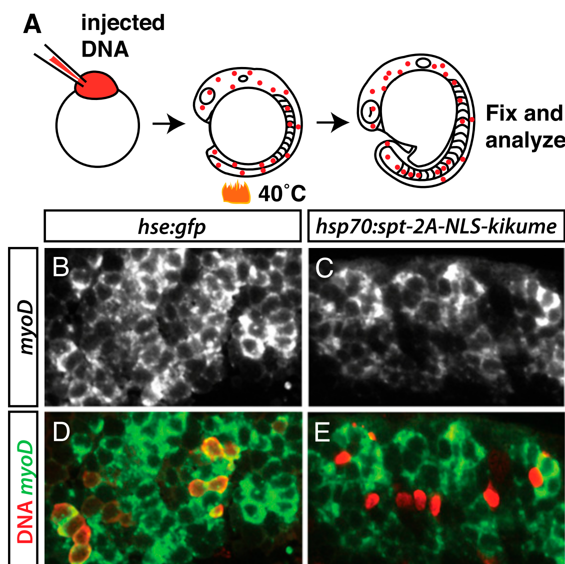

Figure 5. *spt* misexpression inhibits *myoD* expression. (*A*) Diagram depicting mosaic inheritance of injected DNA. Injected embryos were heat-shocked at the 12-somite stage and collected 4 h after heat shock. (*B–E*) Expression of *myoD* is disrupted in cells with injected DNA that drives expression of Spt and NLS-Kikume but not in cells with injected DNA that drives GFP expression alone. *hse:gfp* is a multimerized heat-shock promoter that drives GFP expression.

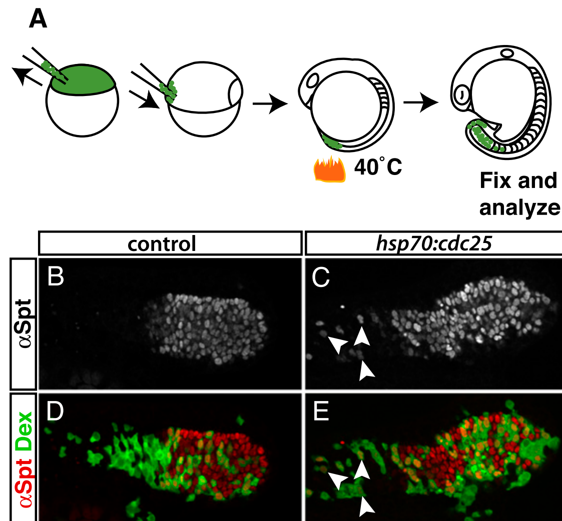

Figure 6. Ectopic Cdc25a has a cell-autonomous effect on Spt. (*A*) Diagram depicting the method for transplant. Cells injected with fluorescent dextran (green) at the one-cell stage were transplanted from a sphere stage embryo to a shield stage embryo and then heat-shocked at the six-somite stage and collected 6 h later. (*B*,*C*) Immunolabeling reveals that the domain of Spt protein extends more anteriorly after ectopic expression of *cdc25a*. (*D*,*E*) Overlay of FITC dextran (which labels transplanted cells) and Spt expression shows that transplanted cells misexpressing Cdc25a ectopically express Spt. Arrowheads highlight three of several cells that ectopically express Spt in the anterior region.

Regulation of Cdc25 activity by phosphorylation

The Cdc25 family is inhibited by several kinases, including Chk1 and Chk2, which can cause 14-3-3 binding, promote degradation, and inhibit interaction with Cyclin–CDK complexes (for review, see Karlsson-Rosenthal and Millar 2006). We considered that the variably penetrant phenotype observed with our *hsp70:cdc25* line might be due to Chk-mediated inhibition of Cdc25. We recently produced a new transgenic line in which three serines and threonines conserved between fish and human Cdc25a that have been shown in other systems to have important regulatory roles were mutated to alanines. In this line (*hsp70:3S/T → A cdc25a*), we found that a single copy of the transgene uniformly produced the strong P3 phenotype (Supplemental Fig. S4), consistent with misexpressed Cdc25a being down-regulated by phosphorylation in our original line. We therefore recommend that all future studies on Cdc25a be done with this new line.

Since the *hsp70:3S/T-A cdc25a* line produced a uniform phenotype when heat-shocked at 40°C, we asked whether lower-temperature heat shocks would produce a partial response, since lower temperatures result in reduced levels of transgene expression. Performing the heat shock at 38°C induced expression of Cdc25a, as seen by fluorescence from the coexpressed Venus, but did not alter the development of the embryo (Supplemental Fig. S4; data not shown). Thus, embryos show an all or nothing response to 3S/T → A Cdc25a, demonstrating that when the conserved phosphorylation sites on Cdc25a are ab-

sent, a specific threshold of Cdc25a activity is required to perturb embryonic development.

Discussion

We show here that proliferation of the posterior progenitor cells is differentially regulated in the two major phases of early development. During the gastrula phase, the posterior progenitors undergo two rapid divisions, quadrupling their number during gastrulation. As somitogenesis begins, proliferation in the progenitors is shut down, and division occurs only when the progenitors begin to differentiate into mesodermal cells. After they are incorporated into somites, cells undergo one more division (data not shown) such that each posterior progenitor at the early gastrula stage produces 16 progeny (Martin and Kimelman 2012). We found that this pattern of division matches the expression of *cdc25a*, which is ubiquitously expressed during gastrulation but then depleted from the bipotential progenitor cells during somitogenesis. *cdc25a* expression at this stage in the early differentiating mesodermal cells is consistent with the round of division the cells undergo once they leave the progenitor zone. Through regulated expression of *cdc25a*, the embryo carefully controls when and where proliferation occurs during the early stages of body formation, which resembles the regulation of mitotic domains during early *Drosophila* development. Our results are broadly consistent with those previously reported by Kanki and Ho (1997), who examined mitotic indices in posterior regions of the embryo. They observed that the most posterior end of the embryo had a twofold lower mitotic index, although because they were not able to distinguish different cell types (bipotential progenitor, prospective neural, and prospective mesodermal) or progenitor cells versus cells starting on the path to differentiation, they were unable to observe the quiescence of the progenitor cells and the division connected to the onset of differentiation. These results emphasize the value of following the proliferation and differentiation trajectory of single cells in a living embryo using photoconvertible proteins as described here.

Why is division compartmentalized such that the bipotential progenitors are quiescent during somitogenesis? Since proliferation involves a rearrangement of the cytoskeleton, one possibility is that mitosis could complicate morphogenetic movements that occur in the tailbud (Kanki and Ho 1997; Lawton et al. 2013), similar to other cases where the function of Cdc25 is regulated to prevent a conflict between cell division and morphogenesis (Grosshans and Wieschaus 2000; Mata et al. 2000; Seher and Leptin 2000; Leise and Mueller 2002; Murakami et al. 2004; Saka and Smith 2004; Ogura et al. 2011). In the progenitor zone, cell division could potentially interfere with signaling or adhesive interactions between the relatively immotile progenitor cells (Lawton et al. 2013), alter the series of morphological changes at the start of differentiation that are regulated in part by Spt (Row et al. 2011), or disrupt the slowing of cell motility that precedes somite formation (Lawton et al. 2013). While we did not investigate morphogenesis in detail, misexpression of Cdc25a

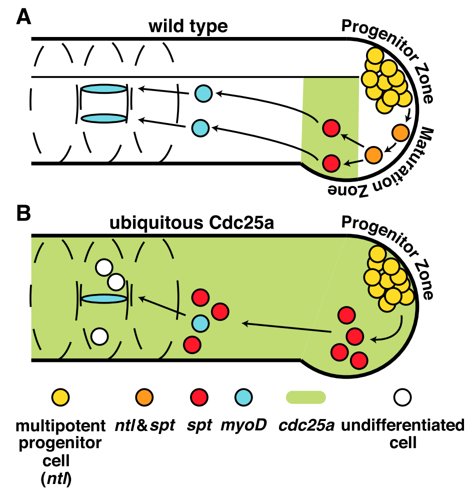

Figure 7. A model depicts quiescence, proliferation, and the role of Cdc25a during somitogenesis. (*A*) Normally, the progenitor cells express *ntl* and only initiate *spt* when they begin to differentiate in the maturation zone. Cells typically express *cdc25a* and divide after they begin to differentiate. After silencing *spt*, cells activate *myoD* (and *myf5*) and then differentiate as muscle. (*B*) Ectopic expression of *cdc25a* during somitogenesis blocks cells from expressing *myoD* (and *myf5*) and forming muscle by maintaining expression of *spt*. Ectopic Cdc25 also causes cells to prematurely inactivate *ntl*, thus eliminating the maturation zone.

does cause defects in the formation of the body, typically observed as an upward bending of the tail (Fig. 3; Supplemental Fig. S4). A second possibility, revealed in a recent analysis of the zebrafish segmentation clock using single-cell labeling, intriguingly revealed that mitosis occurs in the mesodermal precursors during the low phases of *her1* oscillation, which was proposed to be important for propagating synchrony and minimizing the disruption of mitosis on Notch signaling (Delaune et al. 2012). Timing the cell cycle to a period subsequent to the start of mesodermal differentiation could help coordinate the segmentation clock. While embryos continue to form somites after Cdc25a misexpression, there are alterations in the somite boundaries (Fig. 3), and it will be interesting in the future to determine how much of this is due to subtle alterations in *her1* expression.

The cell cycle and differentiation

The major new finding reported here is that quiescence is required by the posterior progenitors to allow the normal process of differentiation from bipotential precursor to differentiated muscle cell. Prematurely driving the cells into mitosis by misexpressing Cdc25 results in embryos with fewer somites and causes a depletion of the number of cells beginning differentiation in the maturation zone (where cells normally express both *ntl* and *spt*) as well as a perdurance of *spt* and *tbx24* expression in the PSM (Fig. 7B). Moreover, we show that continuation of *spt* expression is cell-autonomous and that the maintenance of Spt beyond the most posterior end of the body inhibits

the expression of the essential muscle regulatory factors *myoD* and *myf5*, accounting for the perturbation in muscle development. Because undifferentiated cells are incapable of contributing to myofibers, they would not be expected to contribute substantively to the length of the embryo. Thus, the precise control of the cell cycle by regulating *cdc25* expression is essential for the normal process of muscle differentiation and establishing the proper length of the embryo. While much recent work in embryonic stem cells and *Xenopus* has emphasized the regulation of G1 phase in controlling differentiation (Richard-Parpaillon et al. 2004; Coronado et al. 2013; Pauklin and Vallier 2013), our results reveal that control of G2 exit also plays an essential role in regulating progenitor differentiation.

Why would altering the cell cycle affect the process of differentiation? Large-scale comparison of chromatin between pluripotent and differentiated cells reveals widespread epigenetic and nuclear architecture changes as cells differentiate (Stergachis et al. 2013; Zhang et al. 2013; Zhu et al. 2013). Similarly, as *Drosophila* neuroblasts differentiate, *hunchback* (*hb*) expression is down-regulated, and the *hb* gene is observed to move to the nuclear periphery, a region associated with gene repression (Kohwi et al. 2013). From these results, we suggest that the timing of the cell cycle could be precisely regulated in vivo during differentiation to allow for changes in the epigenetic marks and/or nuclear architecture, which could facilitate maintenance of *ntl* and repression of *spt*, two key early differentiation genes. We speculate that a premature mitosis could be incompatible with chromatin rearrangements necessary for the changes in gene expression as cells pass through the early stages of differentiation. Although analysis of either the nuclear architecture or epigenetic marks in the small group of cells that comprise the tailbud is technically very challenging with current technology, future studies of this type will provide important clues to the links between proliferation and differentiation in vivo.

Conclusion

We showed that cell division is compartmentalized by the regulated expression of *cdc25a* during early development of the zebrafish body and demonstrated that this restricted *cdc25a* expression is critical for muscle differentiation during somitogenesis, establishing a new link between the S/G2 phase of the cell cycle and differentiation from a progenitor population. The Dual Fucci line described here will make it easy to find additional cells held in G2 in adults and at all stages of development, whereas the *hsp70:cdc25* line will allow the role of Cdc25 in these cells to be readily assessed.

Material and methods

Cell labeling and time-lapse imaging

Cells within the posterior progenitor zone on the ventral side of the embryo ~10–30 cells from the margin were targeted for photoconversion using a 5-sec pulse of 405-nm laser light. Static images were collected ~4 h later from live embryos using a Fluoview 1000 laser-scanning confocal microscope (Olympus). Time-lapse images were collected using a spinning disk confocal microscope (3I). For time-lapse imaging, images were collected using a 10× objective at different intervals for gastrulation (every 3 min for 4 h) and somitogenesis (every 6 min for 10 h). Data were analyzed using Slidebook 5.0 (3I). Briefly, three-dimensional (3D) data sets that covered 125 μm were condensed to two dimensions using a maximum intensity projection, and the time that a single cell noticeably split to two cells was recorded as a cell division.

Generation of Dual Fucci and EF1α:Kikume

For the Dual Fucci line, the zGeminin degron (Sugiyama et al. 2009) was cloned downstream from a 3xFlag tag. Flag-Cerulean-zGeminin was then placed upstream of a viral 2A peptide (Provost et al. 2007). The mCherry-zCdt1 fusion protein (Sugiyama et al. 2009) was placed downstream from the 2A peptide and then inserted in a plasmid containing Tol2 elements (Kawakami et al. 2000) and the *ubiquitin* promoter (Mosimann et al. 2011). The plasmid was used to create a stable line as previously described (Kawakami et al. 2000). The Cerulean is shown as green in Figure 1, Supplemental Figure S2, and Supplemental Movie S2 for better contrast with the red. For the EF1α:NLS-Kikume line, Kikume with a nuclear localization signal was placed upstream of a viral 2A peptide and GFP with a CAAX membrane localization sequence. The coding sequence for both fluorescent molecules was placed downstream from the *Xenopus* EF1α promoter (Lin et al. 1994) in a plasmid that contained Tol2 elements and was used to make a stable transgenic line. These transgenic lines and those described below will be available at the Zebrafish International Resource Center.

In situ hybridization

Alkaline phosphatase and fluorescent in situ hybridization (Lauter et al. 2011) were performed as described. 3D projections from fluorescent in situ data were generated using a fixed lighting projection in Slidebook 5.5 (3I).

Generation of hsp70:cdc25 and hsp70:3S/T → A cdc25

Full-length Cdc25a was amplified using the following primers: 5′-CCGGATCCACCATGGATATTGATATGGTTCCAGG and 5′-CCATCGATGGAGTTTTTTGAGACGGCTGTAC. Cdc25a was then cloned into a plasmid with Tol2 elements (Kawakami et al. 2000), a fragment of the zebrafish *hsp70* promoter (Halloran et al. 2000), and the fluorescent protein Venus, separated from Cdc25a by a 2A viral peptide (Provost et al. 2007). *hsp70:3S/T → A cdc25* was created similarly with the exception that S213, S305, and T564 were mutated to alanines using site-directed mutagenesis. The plasmids were used to create stable transgenic lines.

Immunofluorescence, Lysotracker, and phalloidin staining

Primary antibodies used for immunofluorescence were rabbit pH3 (1:500; Abcam), mouse F310 (1:100; Hybridoma Bank, University of Iowa), and mouse F59 (1:10; Hybridoma Bank, University of Iowa). For Lysotracker staining, embryos were heat-shocked and raised for 4 h followed by 1 h in 10 μM Lysotracker Red before being fixed in PFA overnight and stored in MeOH. For phalloidin labeling, embryos were fixed and permeabilized for 1.5 h with 2% Triton X-100 in PBS before incubation in phalloidin 488 or 568 diluted 1:20 in PBT for 1 h at room temperature. For muscle cross-sectional area analysis,

images from phalloidin-stained embryos were imported into Slidebook 5.5 (3I). Cross-sectional images and areas were obtained using the "three view" function.

Cell transplantation

Control Wik/AB or *hsp70:cdc25* embryos were injected with 1% fluorescein dextran. Cells were transplanted from fluorescent sphere stage (4 hpf) donors to the ventral margins of nonfluorescent shield stage (6 hpf) Wik/AB hosts.

Heat-shock treatments

Embryos were heat-shocked by transfer from 28.5°C to a circulating water bath for 30 min at 40°C. Embryos were then placed for at least 30 min at 28.5°C. Animals were handled in accordance with the guidelines of the University of Washington Institutional Animal Care and Use Committee.

Statistical analysis and mitotic index calculation

Mean somite counts, mitotic indices, number of normal somites formed, and mean muscle areas were compared using a Welch's *t*-test that treated each embryo as an independent sample. Mitotic index was calculated by dividing the number of pH3-positive cells by the total number of cells and multiplying by 100.

Acknowledgments

We thank Ben Martin for critical comments on an earlier version of the manuscript and the *hsp70:spt-2A-NLS-kikume* plasmid, Richard Row for advice and discussion, Yu-Hsuan Peng for technical assistance, Dale Hailey for assistance with microscopy, and Lara Backman for help with preliminary results. This work was supported by a National Institutes of Health grant (RO1GM079203) to D.K., and a Ruth Kirschstein National Research Service Award fellowship (GM099306) to C.M.B.

References

Ahn D, You K-H, Kim C-H. 2012. Evolution of the tbx6/16 subfamily genes in vertebrates: Insights from zebrafish. *Mol Biol Evol* **29:** 3959–3983.

Amacher SL, Draper BW, Summers BR, Kimmel CB. 2002. The zebrafish T-box genes no tail and spadetail are required for development of trunk and tail mesoderm and medial floor plate. *Development* **129:** 3311–3323.

Bessarab DA, Chong S-W, Srinivas BP, Korzh V. 2008. Six1a is required for the onset of fast muscle differentiation in zebrafish. *Dev Biol* **323:** 216–228.

Buckingham ME, Meilhac SM. 2011. Tracing cells for tracking cell lineage and clonal behavior. *Dev Cell* **21:** 394–409.

Buckingham M, Vincent SD. 2009. Distinct and dynamic myogenic populations in the vertebrate embryo. *Curr Opin Genet Dev* **19:** 444–453.

Cambray N, Wilson V. 2002. Axial progenitors with extensive potency are localised to the mouse chordoneural hinge. *Development* **129:** 4855–4866.

Cambridge SB, Davis RL, Minden JS. 1997. *Drosophila* mitotic domain boundaries as cell fate boundaries. *Science* **277:** 825–828.

Christ B, Huang R, Scaal M. 2007. Amniote somite derivatives. *Dev Dyn* **236:** 2382–2396.

Cooke J. 1973. Properties of the primary organization field in the embryo of *Xenopus laevis*. IV. Pattern formation and regulation following early inhibition of mitosis. *J Embryol Exp Morphol* **30:** 49–62.

Coronado D, Godet M, Bourillot P-Y, Tapponnier Y, Bernat A, Petit M, Afanassieff M, Markossian S, Malashicheva A, Iacone R, et al. 2013. A short G1 phase is an intrinsic determinant of naïve embryonic stem cell pluripotency. *Stem Cell Res (Amst)* **10:** 118–131.

Dalle Nogare DE, Arguello A, Sazer S, Lane ME. 2007. Zebrafish cdc25a is expressed during early development and limiting for post-blastoderm cell cycle progression. *Dev Dyn* **236:** 3427–3435.

Dalle Nogare DE, Pauerstein PT, Lane ME. 2009. G2 acquisition by transcription-independent mechanism at the zebrafish midblastula transition. *Dev Biol* **326:** 131–142.

Delaune EA, François P, Shih NP, Amacher SL. 2012. Single-cell-resolution imaging of the impact of Notch signaling and mitosis on segmentation clock dynamics. *Dev Cell* **23:** 995–1005.

Devoto SH, Melançon E, Eisen JS, Westerfield M. 1996. Identification of separate slow and fast muscle precursor cells in vivo, prior to somite formation. *Development* **122:** 3371–3380.

DiTalia S, Wieschaus EF. 2012. Short-term integration of Cdc25 dynamics controls mitotic entry during *Drosophila* gastrulation. *Dev Cell* **22:** 763–774.

DiTalia S, She R, Blythe SA, Lu X, Zhang QF, Wieschaus EF. 2013. Posttranslational control of Cdc25 degradation terminates *Drosophila*'s early cell-cycle program. *Curr Biol* **23:** 127–132.

Edgar BA, Datar SA. 1996. Zygotic degradation of two maternal Cdc25 mRNAs terminates *Drosophila*'s early cell cycle program. *Genes Dev* **10:** 1966–1977.

Edgar BA, O'Farrell PH. 1989. Genetic control of cell division patterns in the *Drosophila* embryo. *Cell* **57:** 177–187.

Edgar BA, O'Farrell PH. 1990. The three postblastoderm cell cycles of *Drosophila* embryogenesis are regulated in G2 by string. *Cell* **62:** 469–480.

Farrell JA, O'Farrell PH. 2013. Mechanism and regulation of Cdc25/twine protein destruction in embryonic cell-cycle remodeling. *Curr Biol* **23:** 118–126.

Farrell JA, Shermoen AW, Yuan K, O'Farrell PH. 2012. Embryonic onset of late replication requires Cdc25 down-regulation. *Genes Dev* **26:** 714–725.

Fior R, Maxwell AA, Ma TP, Vezzaro A, Moens CB, Amacher SL, Lewis J, Saúde L. 2012. The differentiation and movement of presomitic mesoderm progenitor cells are controlled by Mesogenin 1. *Development* **139:** 4656–4665.

Foe VE. 1989. Mitotic domains reveal early commitment of cells in *Drosophila* embryos. *Development* **107:** 1–22.

Foe VE, O'Dell GM, Edgar BA. 1993. Mitosis and morphogenesis in the *Drosophila* embryo: Point and counterpoint. In *The development of* Drosophila melanogaster (ed. Bate M), pp. 149–300. Cold Spring Harbor Laboratory Press, Cold Spring Harbor, NY.

Gautier J, Solomon MJ, Booher RN, Bazan JF, Kirschner MW. 1991. cdc25 is a specific tyrosine phosphatase that directly activates $p34^{cdc2}$. *Cell* **67:** 197–211.

Griffin KJ, Kimelman D. 2002. One-Eyed Pinhead and Spadetail are essential for heart and somite formation. *Nat Cell Biol* **4:** 821–825.

Grosshans J, Wieschaus E. 2000. A genetic link between morphogenesis and cell division during formation of the ventral furrow in *Drosophila*. *Cell* **101:** 523–531.

Halloran MC, Sato-Maeda M, Warren JT, Su F, Lele Z, Krone PH, Kuwada JY, Shoji W. 2000. Laser-induced gene expression in specific cells of transgenic zebrafish. *Development* **127:** 1953–1960.

Hammond CL, Hinits Y, Osborn DPS, Minchin JEN, Tettamanti G, Hughes SM. 2007. Signals and myogenic regulatory factors restrict pax3 and pax7 expression to dermomyotome-like tissue in zebrafish. *Dev Biol* **302:** 504–521.

Henry CA, McNulty IM, Durst WA, Munchel SE, Amacher SL. 2005. Interactions between muscle fibers and segment boundaries in zebrafish. *Dev Biol* **287:** 346–360.

Hinits Y, Osborn DPS, Hughes SM. 2009. Differential requirements for myogenic regulatory factors distinguish medial and lateral somitic, cranial and fin muscle fibre populations. *Development* **136:** 403–414.

Hirsinger E, Stellabotte F, Devoto SH, Westerfield M. 2004. Hedgehog signaling is required for commitment but not initial induction of slow muscle precursors. *Dev Biol* **275:** 143–157.

Ho RK, Kane DA. 1990. Cell-autonomous action of zebrafish spt-1 mutation in specific mesodermal precursors. *Nature* **348:** 728–730.

Holley SA. 2007. The genetics and embryology of zebrafish metamerism. *Dev Dyn* **236:** 1422–1449.

Hollway GE, Bryson-Richardson RJ, Berger S, Cole NJ, Hall TE, Currie PD. 2007. Whole-somite rotation generates muscle progenitor cell compartments in the developing zebrafish embryo. *Dev Cell* **12:** 207–219.

Kane DA, Warga RM, Kimmel CB. 1992. Mitotic domains in the early embryo of the zebrafish. *Nature* **360:** 735–737.

Kanki JP, Ho RK. 1997. The development of the posterior body in zebrafish. *Development* **124:** 881–893.

Karlsson-Rosenthal C, Millar JBA. 2006. Cdc25: Mechanisms of checkpoint inhibition and recovery. *Trends Cell Biol* **16:** 285–292.

Kawakami K, Shima A, Kawakami N. 2000. Identification of a functional transposase of the Tol2 element, an Ac-like element from the Japanese medaka fish, and its transposition in the zebrafish germ lineage. *Proc Natl Acad Sci* **97:** 11403–11408.

Kimelman D. 2006. Mesoderm induction: From caps to chips. *Nat Rev Genet* **7:** 360–372.

Kimmel CB, Warga RM. 1987. Cell lineages generating axial muscle in the zebrafish embryo. *Nature* **327:** 234–237.

Kimmel CB, Kane DA, Walker C, Warga RM, Rothman MB. 1989. A mutation that changes cell movement and cell fate in the zebrafish embryo. *Nature* **337:** 358–362.

Kimmel CB, Warga RM, Schilling TF. 1990. Origin and organization of the zebrafish fate map. *Development* **108:** 581–594.

Kohwi M, Lupton JR, Lai S-L, Miller MR, Doe CQ. 2013. Developmentally regulated subnuclear genome reorganization restricts neural progenitor competence in *Drosophila*. *Cell* **152:** 97–108.

Lardelli M. 2003. The evolutionary relationships of zebrafish genes tbx6, tbx16/spadetail and mga. *Dev Genes Evol* **213:** 519–522.

Lauter G, Söll I, Hauptmann G. 2011. Multicolor fluorescent in situ hybridization to define abutting and overlapping gene expression in the embryonic zebrafish brain. *Neural Dev* **6:** 10.

Lawton AK, Nandi A, Stulberg MJ, Dray N, Sneddon MW, Pontius W, Emonet T, Holley SA. 2013. Regulated tissue fluidity steers zebrafish body elongation. *Development* **140:** 573–582.

Leise W, Mueller PR. 2002. Multiple Cdk1 inhibitory kinases regulate the cell cycle during development. *Dev Biol* **249:** 156–173.

Lin S, Yang S, Hopkins N. 1994. lacZ expression in germline transgenic zebrafish can be detected in living embryos. *Dev Biol* **161:** 77–83.

Martin BL, Kimelman D. 2008. Regulation of canonical Wnt signaling by Brachyury is essential for posterior mesoderm formation. *Dev Cell* **15:** 121–133.

Martin BL, Kimelman D. 2010. Brachyury establishes the embryonic mesodermal progenitor niche. *Genes Dev* **24:** 2778–2783.

Martin BL, Kimelman D. 2012. Canonical Wnt signaling dynamically controls multiple stem cell fate decisions during vertebrate body formation. *Dev Cell* **22:** 223–232.

Mata J, Curado S, Ephrussi A, Rørth P. 2000. Tribbles coordinates mitosis and morphogenesis in *Drosophila* by regulating string/CDC25 proteolysis. *Cell* **101:** 511–522.

Maves L, Waskiewicz AJ, Paul B, Cao Y, Tyler A, Moens CB, Tapscott SJ. 2007. Pbx homeodomain proteins direct Myod activity to promote fast-muscle differentiation. *Development* **134:** 3371–3382.

Mosimann C, Kaufman CK, Li P, Pugach EK, Tamplin OJ, Zon LI. 2011. Ubiquitous transgene expression and Cre-based recombination driven by the ubiquitin promoter in zebrafish. *Development* **138:** 169–177.

Murakami MS, Moody SA, Daar IO, Morrison DK. 2004. Morphogenesis during *Xenopus* gastrulation requires Wee1-mediated inhibition of cell proliferation. *Development* **131:** 571–580.

Nikaido M, Kawakami A, Sawada A, Furutani-Seiki M, Takeda H, Araki K. 2002. Tbx24, encoding a T-box protein, is mutated in the zebrafish somite-segmentation mutant fused somites. *Nat Genet* **31:** 195–199.

Oates AC, Morelli LG, Ares S. 2012. Patterning embryos with oscillations: Structure, function and dynamics of the vertebrate segmentation clock. *Development* **139:** 625–639.

Ogura Y, Sakaue-Sawano A, Nakagawa M, Satoh N, Miyawaki A, Sasakura Y. 2011. Coordination of mitosis and morphogenesis: Role of a prolonged G2 phase during chordate neurulation. *Development* **138:** 577–587.

Pauklin S, Vallier L. 2013. The cell-cycle state of stem cells determines cell fate propensity. *Cell* **155:** 135–147.

Pourquié O. 2011. Vertebrate segmentation: From cyclic gene networks to scoliosis. *Cell* **145:** 650–663.

Provost E, Rhee J, Leach SD. 2007. Viral 2A peptides allow expression of multiple proteins from a single ORF in transgenic zebrafish embryos. *Genesis* **45:** 625–629.

Richard-Parpaillon L, Cosgrove RA, Devine C, Vernon AE, Philpott A. 2004. G1/S phase cyclin-dependent kinase overexpression perturbs early development and delays tissue-specific differentiation in *Xenopus*. *Development* **131:** 2577–2586.

Robu ME, Larson JD, Nasevicius A, Beiraghi S, Brenner C, Farber SA, Ekker SC. 2007. p53 activation by knockdown technologies. *PLoS Genet* **3:** e78.

Row RH, Maître J-L, Martin BL, Stockinger P, Heisenberg C-P, Kimelman D. 2011. Completion of the epithelial to mesenchymal transition in zebrafish mesoderm requires Spadetail. *Dev Biol* **354:** 102–110.

Russell P, Nurse P. 1986. $cdc25^+$ functions as an inducer in the mitotic control of fission yeast. *Cell* **45:** 145–153.

Saka Y, Smith JC. 2004. A *Xenopus* tribbles orthologue is required for the progression of mitosis and for development of the nervous system. *Dev Biol* **273:** 210–225.

Sakaue-Sawano A, Kurokawa H, Morimura T, Hanyu A, Hama H, Osawa H, Kashiwagi S, Fukami K, Miyata T, Miyoshi H, et al. 2008. Visualizing spatiotemporal dynamics of multicellular cell-cycle progression. *Cell* **132:** 487–498.

Schier AF, Talbot WS. 2005. Molecular genetics of axis formation in zebrafish. *Annu Rev Genet* **39:** 561–613.

Schulte-Merker S, van Eeden FJ, Halpern ME, Kimmel CB, Nusslein-Volhard C. 1994. no tail (ntl) is the zebrafish homologue of the mouse T (Brachyury) gene. *Development* **120:** 1009–1015.

Seher TC, Leptin M. 2000. Tribbles, a cell-cycle brake that coordinates proliferation and morphogenesis during *Drosophila* gastrulation. *Curr Biol* **10:** 623–629.

Shimuta K, Nakajo N, Uto K, Hayano Y, Okazaki K, Sagata N. 2002. Chk1 is activated transiently and targets Cdc25A for degradation at the *Xenopus* midblastula transition. *EMBO J* **21:** 3694–3703.

Stellabotte F, Dobbs-McAuliffe B, Fernández DA, Feng X, Devoto SH. 2007. Dynamic somite cell rearrangements lead to distinct waves of myotome growth. *Development* **134:** 1253–1257.

Stergachis AB, Neph S, Reynolds A, Humbert R, Miller B, Paige SL, Vernot B, Cheng JB, Thurman RE, Sandstrom R, et al. 2013. Developmental fate and cellular maturity encoded in human regulatory DNA landscapes. *Cell* **154:** 888–903.

Sugiyama M, Sakaue-Sawano A, Iimura T, Fukami K, Kitaguchi T, Kawakami K, Okamoto H, Higashijima S, Miyawaki A. 2009. Illuminating cell-cycle progression in the developing zebrafish embryo. *Proc Natl Acad Sci* **106:** 20812–20817.

Szeto DP, Kimelman D. 2006. The regulation of mesodermal progenitor cell commitment to somitogenesis subdivides the zebrafish body musculature into distinct domains. *Genes Dev* **20:** 1923–1932.

Tam PP. 1981. The control of somitogenesis in mouse embryos. *J Embryol Exp Morphol* **65:** 103–128.

Tapscott SJ. 2005. The circuitry of a master switch: Myod and the regulation of skeletal muscle gene transcription. *Development* **132:** 2685–2695.

Tsutsui H, Karasawa S, Shimizu H, Nukina N, Miyawaki A. 2005. Semi-rational engineering of a coral fluorescent protein into an efficient highlighter. *EMBO Rep* **6:** 233–238.

Tzouanacou E, Wegener A, Wymeersch FJ, Wilson V, Nicolas JF. 2009. Redefining the progression of lineage segregations during mammalian embryogenesis by clonal analysis. *Dev Cell* **17:** 365–376.

Verduzco D, Dovey JS, Shukla AA, Kodym E, Skaug BA, Amatruda JF. 2012. Multiple isoforms of CDC25 oppose ATM activity to maintain cell proliferation during vertebrate development. *Mol Cancer Res* **10:** 1451–1461.

Warga RM, Nusslein-Volhard C. 1999. Origin and development of the zebrafish endoderm. *Development* **126:** 827–838.

Wilson V, Olivera-Martinez I, Storey KG. 2009. Stem cells, signals and vertebrate body axis extension. *Development* **136:** 1591–1604.

Yabe T, Takada S. 2012. Mesogenin causes embryonic mesoderm progenitors to differentiate during development of zebrafish tail somites. *Dev Biol* **370:** 213–222.

Zhang L, Kendrick C, Julich D, Holley SA. 2008. Cell cycle progression is required for zebrafish somite morphogenesis but not segmentation clock function. *Development* **135:** 2065–2070.

Zhang Y, Wong C-H, Birnbaum RY, Li G, Favaro R, Ngan CY, Lim J, Tai E, Poh HM, Wong E, et al. 2013. Chromatin connectivity maps reveal dynamic promoter-enhancer long-range associations. *Nature* **504:** 306–310.

Zhu J, Adli M, Zou JY, Verstappen G, Coyne M, Zhang X, Durham T, Miri M, Deshpande V, De Jager PL, et al. 2013. Genome-wide chromatin state transitions associated with developmental and environmental cues. *Cell* **152:** 642–654.